

Rapidity distributions of pions in p+p and Pb+Pb collisions at CERN SPS energies

Andrzej Rybicki¹, Antoni Szczurek^{1,2}, Mirosław Kielbowicz¹, Antoni Marcinek¹, Vitalii Ozvenchuk¹, Łukasz Rozpłochowski³

¹ H. Niewodniczański Institute of Nuclear Physics, Polish Academy of Sciences, Radzikowskiego 152, 31-342 Kraków, Poland

² University of Rzeszów, Rejtana 16, 35-959 Rzeszów, Poland

³ Jagiellonian University, Kraków, Poland

Abstract

The centrality dependence of rapidity distributions of pions in Pb+Pb reactions can be understood by imposing local energy-momentum conservation in the longitudinal “fire-streaks” of excited matter. With no tuning nor adjustment to the experimental data, the rapidity distribution of pions produced by the fire-streak which we obtained from Pb+Pb collisions reproduces the shape of the experimental pion rapidity distribution in p+p interactions, measured by the NA49 Collaboration at the same energy. The observed difference in the absolute normalization of this distribution can be explained by the difference in the overall energy balance, induced by baryon stopping and strangeness enhancement phenomena occurring in heavy ion collisions. We estimate the latter effects using a collection of SPS experimental data on π^\pm , K^\pm , net p , and n production in p+p and Pb+Pb reactions. Implications of the above findings are discussed.

I. INTRODUCTION

In our recent paper on the implications of energy and momentum ($E-\vec{p}$) conservation for heavy ion collisions at CERN SPS energies [1] we formulated a simple model for the longitudinal evolution of the participant system. This model, with some degree of similarity to the fire-streak approach of Refs [2], assumed local $E-\vec{p}$ conservation in the plane perpendicular to the collision axis and consequently, formation and independent fragmentation of finite volumes of excited primordial matter (“fire-streaks”) into finite state particles. The kinematical characteristics (rapidity, invariant mass) of the fire-streaks were directly given by the $E-\vec{p}$ conservation. We did not address the exact physical nature of the fire-streaks although to think about color string conglomerates or initial volume elements of quark-gluon plasma would not seem unnatural. With a simple, three-parameter fire-streak fragmentation function ensuring energy conservation, our model provided a surprisingly good description of the whole centrality dependence of negative pion dn/dy distributions in Pb+Pb reactions at $\sqrt{s_{NN}} = 17.3$ GeV, measured by the NA49 experiment [5]. A reminder of the model is presented in Fig. 1, while a compilation of results is shown in Fig. 2. It is noticeable that the model explains *both* the evolution of absolutely normalized π^- yields and of the distribution’s shape as a function of centrality. In Fig. 3 we present the result of a first test of our model for Pb+Pb collisions at a lower SPS energy, $\sqrt{s_{NN}} = 8.8$ GeV. The overall similarity of this result to that shown in Fig. 2(b) suggests the applicability of our model to pion production in some extended range of collision energy, 8.8-17.3 GeV at the least.

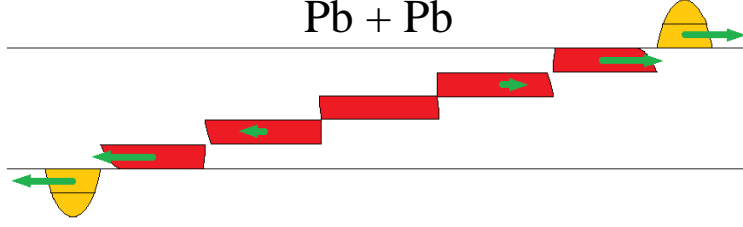


FIG. 1:
A schematic picture of our model of Pb+Pb collisions [1].

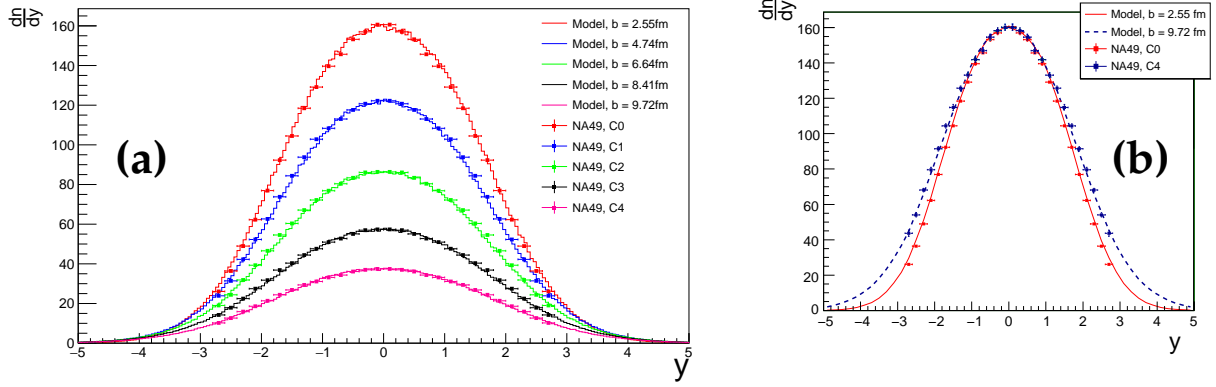


FIG. 2:
(a) Rapidity distributions of π^- mesons in centrality selected Pb+Pb collisions at top SPS energy, $\sqrt{s_{NN}} = 17.3$ GeV, together with our model calculations [1], (b) change of width of the π^- distribution from peripheral to central Pb+Pb collisions at $\sqrt{s_{NN}} = 17.3$ GeV, and its description by our model [1]. In panel (b), for peripheral collisions, the experimental data and model curves have been scaled up to fit the same maximum as for central collisions.

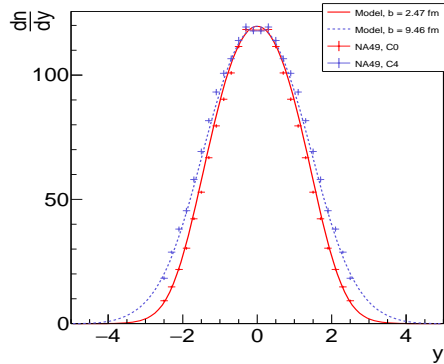


FIG. 3:
Change of width of the π^- rapidity distribution from peripheral to central Pb+Pb collisions at the energy $\sqrt{s_{NN}} = 8.8$ GeV, and its description by our model [1]. For peripheral collisions, the experimental data and model curves have been scaled up to fit the same maximum as for central collisions. The experimental data points come from the NA49 experiment [5].

We interpreted the success of our simple model as a hint that energy-momentum conservation indeed plays a dominant role in the longitudinal evolution of the system created in A+A collisions, at SPS energy. Now we wish to compare the results of our work on Pb+Pb collisions to more elementary p+p reactions. The question whether the non-perturbative dynamical mechanisms governing the latter are qualitatively similar or different from those in heavy ion reactions is a long-standing one. Evident differences on the quantitative level, including in particular the enhancement of strangeness production and its energy dependence [6], were interpreted as onset of deconfinement and transition to quark-gluon plasma [7, 8]. On the other hand, qualitative similarities between p+p and Pb+Pb reactions at SPS [9] and LHC energies [10] still constitute a challenge for phenomenological models (see, e.g., [11]). We find it therefore a key question to verify how our simple energy-momentum conservation picture in A+A reactions compares to proton-proton collisions.

This paper is organized as follows. In section II we remind the basic formulae defining our fire-streak fragmentation function. A comparison between the latter and p+p data from the NA49 Collaboration is made in section III. The problem of isospin differences between p+p and Pb+Pb collisions is addressed in section IV. Section V includes the analysis of normalization. The implications of our study are discussed in section VI and the summary is made in section VII.

We note that in all the subsequent parts of this paper, we use the formulation “fire-streaks” or “fire-streak approach” to address our earlier work made for A+A collisions [1]. This is made to underline the basic similarity of our approach to the original fire-streak concept of [2]. We note that differences exist on the detailed level, which become clearly apparent from the comparison of our model formulation in section II to the cited original works.

Finally, we also note the correspondence of our results to the recent works aimed at the explanation of Λ and $\bar{\Lambda}$ polarizations observed by the STAR Collaboration in Au+Au collisions [12], by the initial angular momentum generated in a fire-streak-like approach [13]. How the initial angular momentum is transferred to $\Lambda/\bar{\Lambda}$ baryons is still unclear. It is our hope that the work presented here will bring its modest contribution to a better understanding of the applicability of the fire-streak-like approaches to the field of high energy reactions.

II. THE FIRE-STREAK FRAGMENTATION FUNCTION

The model we formulated for ultrarelativistic Pb+Pb collisions, Fig. 1, assumed the division of the 3D nuclear mass distribution into longitudinal “bricks” in the perpendicular plane of the reaction, and the subsequent formation of fire-streaks moving along the collision axis [1]. In the cited reference fire-streaks of finite transverse size, $1 \times 1 \text{ fm}^2$, were considered. Our fire-streak fragmentation function into negative pions was parametrized in the form:

$$\frac{dn}{dy}(y, y_s, E_s^*, m_s) = A \cdot (E_s^* - m_s) \cdot \exp\left(-\frac{[(y - y_s)^2 + \epsilon^2]^{\frac{1}{2}}}{r\sigma_y^r}\right) . \quad (2.1)$$

The formula (2.1) defines the distribution $\frac{dn}{dy}$ of negative pions created by the fragmentation of a single fire-streak. We named it “fire-streak fragmentation function” in order

to differentiate from the “standard” parton-to-hadron fragmentation function (FF) [3]. In the above, y is the rapidity of the pion, y_s is the fire-streak rapidity given by energy-momentum conservation, E_s^* is its total energy in its own rest frame (or equivalently, its invariant mass, also given by the $E-\vec{p}$ conservation), and m_s is the sum of “cold” rest masses of the two “bricks” forming the fire-streak (given by collision geometry). ϵ is a small number ensuring the continuity of derivatives ($\epsilon = 0.01$ was used in [1]). Finally, A , σ_y and r are the only free parameters of the function (2.1). They appeared common to all the fire-streaks in all the collisions, and independent of Pb+Pb collision centrality¹. The fit made in our analysis of the NA49 centrality selected Pb+Pb data at $\sqrt{s_{NN}} = 17.3$ GeV [5] gave $A = 0.05598$, $\sigma_y = 1.475$, and $r = 2.55$. In this analysis, our modelled pion rapidity distribution in a given centrality selected sample of Pb+Pb collisions of impact parameter b was constructed as the sum of independent fragmentation functions, corresponding to all the constituent fire-streaks:

$$\frac{dn}{dy}(y, b) = \sum_{(i,j)} \frac{dn}{dy} \left(y, y_{s(i,j)}(b), E_{s(i,j)}^*(b), m_{s(i,j)}(b) \right) , \quad (2.2)$$

where (i,j) denominate the position of a given fire-streak in the transverse (x, y) plane of the Pb+Pb collision. Using formula (2.2), our simple model was able to describe the whole centrality dependence of negative pion dn/dy yields as a function of rapidity, including in particular the narrowing of the rapidity distribution from peripheral to central Pb+Pb collisions as illustrated in Fig. 2.

Now we proceed to proton-proton collisions, where the total available energy is \sqrt{s} . We will naively try to apply the function (2.1) to pion production in the entire p+p system, with $E_s^* \rightarrow \sqrt{s}$, $m_s \rightarrow 2m_p$. The pion rapidity distribution would then be:

$$\frac{dn}{dy} = A \cdot (\sqrt{s} - 2m_p) \cdot \exp \left(- \frac{[y^2 + \epsilon^2]^{\frac{r}{2}}}{r\sigma_y^r} \right) , \quad (2.3)$$

where $\sqrt{s} = 17.27$ GeV as for Pb+Pb collisions, and m_p is the proton mass. We note that $y_s = 0$ by definition in the p+p c.m. system. Applying $\epsilon = 0.01$ and the same parameters $A = 0.05598$, $\sigma_y = 1.475$, and $r = 2.55$ which we obtained from the fit to Pb+Pb collisions [1], we get explicitly:

$$\frac{dn}{dy} \equiv f(y) = 0.8618 \cdot \exp \left(- \frac{[y^2 + 0.01^2]^{\frac{2.55}{2}}}{2.55 \cdot 1.475^{2.55}} \right) . \quad (2.4)$$

In the following section we will directly compare the function (2.4) to the experimental rapidity distribution in p+p collisions. We will constantly address $f(y)$ as “fire-streak fragmentation function” in the text below, to underline that it was deduced from Pb+Pb reactions as described above.

¹ Deviations from the mean value of A quoted above were smaller or comparable to systematical errors of the experimental data [5]. We note that the numerical values of the parameters discussed in the text apply only to the collision energy $\sqrt{s_{NN}} = 17.3$ GeV. The energy dependence of the fire-streak fragmentation function and its parameters, which emerges from the comparison of Figs 2 and 3 is discussed in detail in Appendix B.

III. THE NEGATIVE PION RAPIDITY SPECTRUM

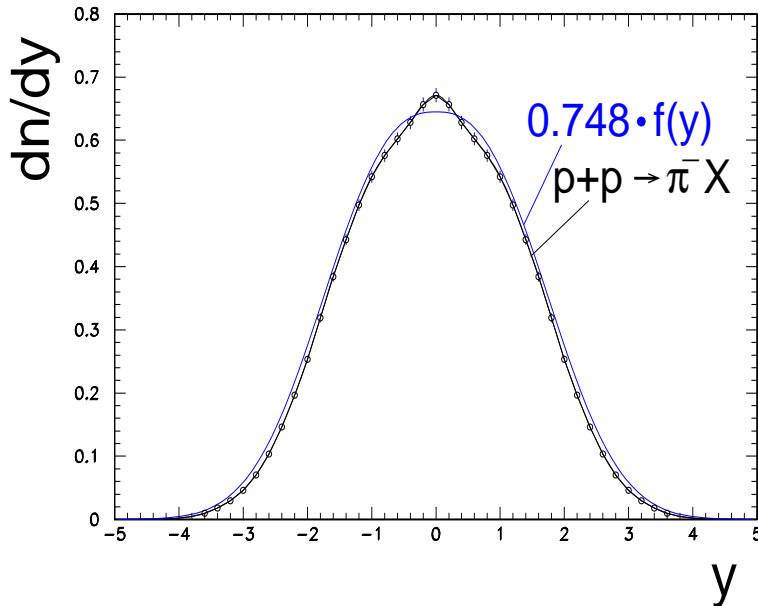


FIG. 4:

Rapidity distribution of negative pions produced in inclusive inelastic $p+p$ collisions at $\sqrt{s} = 17.27$ GeV (experimental data points), compared to our function $f(y)$ from Eq. (2.4) multiplied by 0.748 (blue curve). The data points come from [4] (their numerical values and errors are taken from [14]; only statistical errors are shown). At negative rapidity reflected data points are drawn.

The NA49 experiment published rapidity distributions of positively and negatively charged pions in inclusive inelastic $p+p$ collisions at $\sqrt{s} = 17.27$ GeV [4]. A comparison of shapes between the experimental $p + p \rightarrow \pi^- X$ distribution and our function $f(y)$ defined by Eq. (2.4) above is presented in Fig. 4. We note that the function $f(y)$ multiplied by a factor of 0.748 matches the experimental data reasonably well. Several facts are noteworthy:

- (1.) It is important to underline that the $p + p \rightarrow \pi^- X$ data in Fig. 4 are compared to the *single* fire-streak fragmentation function $f(y)$. This is very different from our study of Pb+Pb collisions made in [1] and shown in Figs 1-3. In this latter case our model calculation was always the *sum* of fragmentation functions corresponding to the different fire-streaks, see Eq. (2.2). Summing over many fire-streaks with different values of rapidity y_S affected the width of the overall pion rapidity distribution, which was largest in peripheral and smallest in central Pb+Pb collisions, see Figs 2-3.

- (2.) Account taken that all the parameters characterizing the function $f(y)$ have been directly inherited from the fit to Pb+Pb collisions,² and account taken of the difference between the two analyses stated in (1.), the overall agreement of the fire-streak functional shape with the experimental p+p data is in our opinion surprisingly good.
- (3.) Notwithstanding the above, a deviation of the data points from $f(y)$ can be seen in the central region (most evidently at $y = 0$). This goes beyond the statistical errors of the data points. It is always tempting to discuss such differences in the context of systematical errors of the experimental p+p and Pb+Pb data [4, 5], but it is more natural to explain them by addressing the limitations of the procedure for the extraction of the fire-streak fragmentation function which we proposed in [1]. Indeed, this function is the result of a non-perturbative process and is only approximated, in an effective way, by our simple formula (2.1). Therefore, its extraction from experimental distributions in Pb+Pb collisions, each being a sum of independent fire-streaks according to Eq. (2.2), will smear out all the “subtleties” present in the shape of $f(y)$, leaving only its basic smoothed form which can be described by Eq. (2.1) and thus giving the result which we see in Fig. 4.
- (4.) Finally, a clear discrepancy in the absolute normalization of our function $f(y)$ with respect to the experimental p+p data is evident from Fig. 4. This discrepancy, which we attribute to baryon stopping and strangeness enhancement phenomena, will be addressed in section V.

The situation described above, and most of all the somewhat intriguing fact that the experimental $p + p \rightarrow \pi^- X$ distribution can be described, or approximated, by the same shape as that obtained in $Pb + Pb \rightarrow \pi^- X$ reactions but for the single fire-streak (item (2.)), raises interesting questions. Some of these will be addressed in the subsequent parts of this paper. In the following two sections we will focus on the difference in absolute normalization discussed in item (4.).

IV. CORRECTION FOR ISOSPIN IN P+P REACTIONS

As we specified in the precedent section, the single fire-streak fragmentation function agrees with the experimental $p + p \rightarrow \pi^- X$ distribution up to a normalization factor of 0.748. Before addressing what we consider as truly dynamical reasons for this difference in normalization, a more “trivial” issue is to be addressed. This is the difference in the isospin content of the p+p and Pb+Pb systems. As the Pb ($A=208, Z=82$) nucleus consists of $\frac{Z}{A}=39.4\%$ protons and $(1 - \frac{Z}{A})=60.6\%$ neutrons, the proper reference for the $Pb+Pb \rightarrow \pi^- X$ spectrum is not the $p+p \rightarrow \pi^- X$ distribution, but rather that of negative pions obtained from a properly averaged mixture of p+p, n+p, p+n, and n+n collisions. This problem is non-negligible at SPS energies where π^+ and π^- yields in p+p collisions differ quite significantly, as shown in Fig. 5.

We address this issue by estimating the proper isospin-averaged distribution following the approach proposed in [15], invoking isospin symmetry in pion production for

² We note that the numerical values of ϵ , σ_y and r as well as the functional shape given by Eq. (2.1) were published in [1] before we started the present analysis.

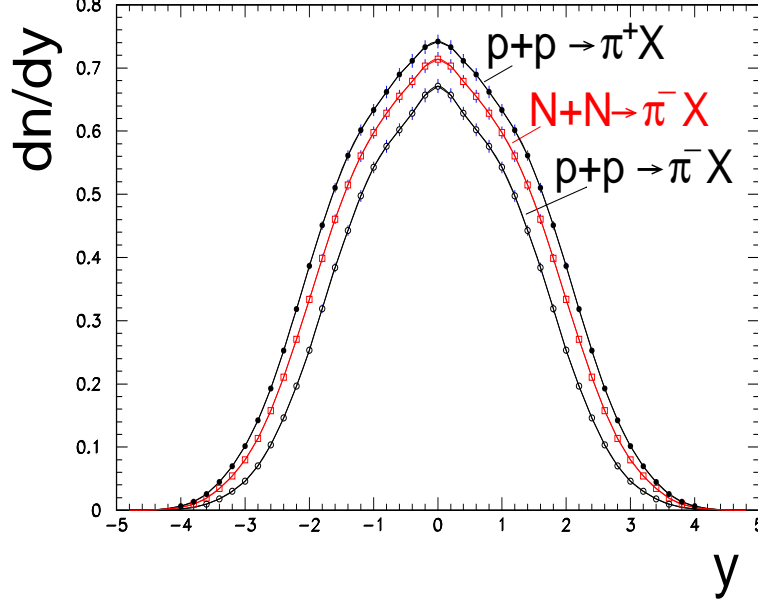


FIG. 5:

Experimental rapidity distributions of positive and negative pions produced in inclusive inelastic p+p collisions at $\sqrt{s} = 17.27$ GeV (black), together with our isospin-averaged negative pion distribution, $N+N \rightarrow \pi^- X$, given by Eq. (4.1) (red). The experimental data points come from [4] (their numerical values and errors are taken from [14] and the same relative errors are assumed for the isospin-averaged distribution). At negative rapidity reflected data points are drawn.

participating protons and neutrons $\left(\frac{dn}{dy}(n \rightarrow \pi^-) = \frac{dn}{dy}(p \rightarrow \pi^+) \right)$. On that basis the proper “nucleon+nucleon” reference for Pb+Pb collisions reads:

$$\frac{dn}{dy}(N + N \rightarrow \pi^- X) = \left(\frac{Z}{A} \right) \cdot \frac{dn}{dy}(p + p \rightarrow \pi^- X) + \left(1 - \frac{Z}{A} \right) \cdot \frac{dn}{dy}(p + p \rightarrow \pi^+ X) \quad . \quad (4.1)$$

The distribution (4.1) is presented in Fig. 5. In Fig. 6, its shape is compared to our function $f(y)$ given by Eq. (2.4). We consider that after the correction for isospin differences, the agreement of the $N + N \rightarrow \pi^- X$ distribution with $f(y)$ - the latter being inherited from our description of the Pb+Pb reactions as explained in section II - is invariably good. The normalization factor increases from 0.748 to 0.812.

In the next section we will attempt to understand this factor.

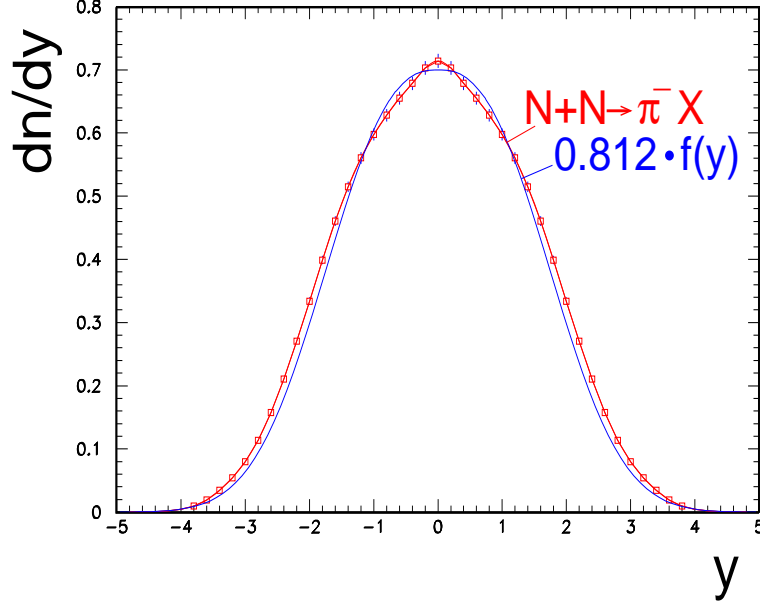


FIG. 6:

Comparison of negative pion rapidity distribution in inclusive inelastic p+p collisions after correction for isospin effects (red points) to our single fire-streak fragmentation function $f(y)$ from Eq. (2.4) (blue curve). The isospin-averaged negative pion distribution $N+N \rightarrow \pi^- X$ is the same as in Fig. 5. Our function $f(y)$ is multiplied by 0.812.

V. THE ABSOLUTELY NORMALIZED PION YIELD IN P+P COLLISIONS

In the following we will use energy conservation to estimate whether the agreement apparent in the comparison of the distribution shapes, in Figs 4 and 6, can be reconciled with the fact that our function $f(y)$, derived from Pb+Pb reactions, brings a total pion yield which is evidently higher than what is measured in p+p collisions. This difference in total pion yield is quantified (after correction for isospin effects) by the normalization factor 0.812 addressed above. We consider it conceivable that specific dynamical mechanisms, similar in p+p and Pb+Pb collisions (dressing up of quarks into hadrons to quote the first example) would lead to a similar *shape* of longitudinal distributions of final state particles, while the absolutely normalized final production *yields* would be significantly different. Therefore we will consider the differences in the overall energy balance between nucleon-nucleon and nucleus-nucleus reactions, that is, the different repartition of collision energy into the various types of final state particles.

We see two main, experimentally well established, phenomena which modify this energy balance. These are:

- (1.) Baryon stopping [16], i.e. the change in baryon inelasticity between p+p and Pb+Pb collisions;
- (2.) Strangeness enhancement, that is the enhanced production of strange over non-strange particle production, since a long time interpreted as connected to quark gluon plasma formation in heavy ion reactions [7].

The influence of these two phenomena on the overall energy repartition in p+p and

Pb+Pb reactions will be estimated below. We underline that the aim of this section is to provide both estimates in a maximally model-independent way. For this reason, we decide not to use any particular model for baryon stopping or strangeness enhancement which would need to be validated against experimental data. Instead, we decide to study these issues using experimental data directly, whenever available. As this will become apparent below, the fact that such a study can be made with a reasonable precision speaks very well for the completeness of experimental information at SPS energy.

Consequently, the work described in sections V A and V B is to be understood as an attempt at a fair comparison of the results of our work on Pb+Pb collisions with experimental p+p data as we said in section I, and not as an extension of the fire-streak model of Pb+Pb collisions to p+p reactions.

A. Baryon stopping

Uniquely for clarity and conciseness, the discussion made below will *implicitly* include the correction for isospin differences between p+p and Pb+Pb reactions addressed in section III above. Thus we will assume that formula (4.1) correctly describes the mixture of nucleon+nucleon (p+p, n+p, p+n and n+n) collisions representative for Pb+Pb reactions, and concisely write

$$\frac{dn}{dy}(p+p) \quad \text{instead of} \quad \frac{dn}{dy}(N+N \rightarrow \pi^- X) \quad (5.1)$$

for the representative, isospin corrected distribution from Eq. (4.1). Consequently whenever we refer to “p+p” (or “pp”) reactions, the representative set of nucleon+nucleon collisions will be meant. Also, we will neglect the small difference between proton and neutron masses. Finally, for simplicity, we will apply the convention $\sqrt{s_{NN}} \equiv \sqrt{s}$ independently on the considered reaction type.

Let us now consider the agreement of rapidity distribution shapes shown in Fig. 6, together with our formulae (2.3) and (2.4). Approximately, we can quantify this agreement as follows:

$$\frac{dn}{dy}(p+p) = A_{pp} \cdot (\sqrt{s} - 2m_p) \cdot \exp\left(-\frac{[y^2 + \epsilon_{AA}^2]^{\frac{r_{AA}}{2}}}{r_{AA} \cdot \sigma_{y_{AA}}^{r_{AA}}}\right) \quad , \quad (5.2)$$

where we put explicitly $\epsilon_{AA} = 0.01$, $\sigma_{y_{AA}} = 1.475$, and $r_{AA} = 2.55$ to underline that these parameters are obtained from AA (Pb+Pb) reactions with no further tuning to p+p collisions. On the other hand the normalization parameter A_{pp} is specific to the p+p reactions. We know from Fig. 6 that

$$A_{pp} = 0.812 \cdot A_{AA} \approx 0.8 \cdot A_{AA} \quad , \quad (5.3)$$

where $A_{AA} = 0.05598$ was obtained from experimental data on Pb+Pb collisions as specified in section II.

Let us now consider a central Pb+Pb collision at impact parameter $b \approx 0$. As it can be immediately seen from the energy-momentum conservation considerations made in our earlier work [1], our model predicts, for such a collision, the formation of fire streaks - all of them build of symmetric “bricks” of equal mass and being at rest in the collision

c.m. system ($y_s \approx 0$). For any given fire-streak made of two bricks of equal mass M the outgoing π^- distribution will be, from Eq. (2.1):

$$\begin{aligned}
\frac{dn}{dy}(A + A \rightarrow \pi^- X) &\equiv \frac{dn}{dy}(A + A) = A_{AA} \cdot (E_s^* - m_s) \cdot \exp\left(-\frac{[(y - y_s)^2 + \epsilon_{AA}^2]^{\frac{r_{AA}}{2}}}{r_{AA} \cdot \sigma_{y_{AA}}^{r_{AA}}}\right) \\
&= A_{AA} \cdot (E_s^* - m_s) \cdot \exp\left(-\frac{[y^2 + \epsilon_{AA}^2]^{\frac{r_{AA}}{2}}}{r_{AA} \cdot \sigma_{y_{AA}}^{r_{AA}}}\right) \\
&= A_{AA} \cdot (M/m_p \cdot \sqrt{s} - 2M) \cdot F_{AA}(y) \\
&= A_{AA} \cdot B_M \cdot (\sqrt{s} - 2m_p) \cdot F_{AA}(y) \quad ,
\end{aligned} \tag{5.4}$$

where we introduced the shape factor $F_{AA}(y) = \exp(-[y^2 + \epsilon_{AA}^2]^{r_{AA}/2} / (r_{AA} \cdot \sigma_{y_{AA}}^{r_{AA}}))$. We note that $B_M = M/m_p$ is the baryon number of each "brick" (equivalent to the number of participating nucleons per fm² in the plane perpendicular to the collision axis). For p+p collisions we rewrite Eq. (5.2) in the same form as (5.4):

$$\frac{dn}{dy}(p + p) = A_{pp} \cdot B_M \cdot (\sqrt{s} - 2m_p) \cdot F_{AA}(y) \quad , \tag{5.5}$$

where $B_M = M/m_p = 1$ for p+p reactions.

Let us now relate the energy available for particle production per incoming nucleon pair, to the outgoing baryon inelasticity K [20] in the final state of the collision:

$$K = \frac{2 \cdot E_{inel}}{\sqrt{s} - 2m_p} \quad , \tag{5.6}$$

where E_{inel} is the total energy lost by the incoming baryon which remains available for particle production. Let us first assume that the available energy repartition between the different types of produced particles (that is, π^+ , π^- , π^0 , kaons, etc) remains the same between (isospin-corrected) p+p and Pb+Pb collisions³. Then we have for the rapidity distribution of negative pions, respectively from Eqs. (5.5) and (5.4):

$$dn/dy(p + p) = B_M \cdot \tilde{A} \cdot 2E_{inel} \cdot F_{AA}(y) \quad , \tag{5.7}$$

$$dn/dy(A + A) = B_M \cdot \tilde{A} \cdot 2E_{inel} \cdot F_{AA}(y) \quad , \tag{5.8}$$

where \tilde{A} is now assumed to be a *constant* factor. From (5.4), (5.5), (5.7), and (5.8) we have:

$$A_{pp} = \tilde{A} \cdot K_{pp} \quad , \tag{5.9}$$

$$A_{AA} = \tilde{A} \cdot K_{AA} \quad . \tag{5.10}$$

Thus under the assumption made above, the difference in normalization of pion rapidity distributions in proton-proton reactions and in a single fire-streak from the Pb+Pb collisions (Figs 4 and 6) would come from differences in final state baryon inelasticity.

Here a lot of information is available at SPS energies. For *proton-proton reactions*, the common knowledge in the community is that the proton loses about half of its energy

³ This assumption will be re-discussed in sections V B and V C.

Reaction	$p + p \rightarrow (p - \bar{p})X$	$p + p \rightarrow (B - \bar{B})X$	$Pb + Pb \rightarrow (p - \bar{p})X$
Ref.	[14, 17]	[14, 17]	[20]
K	0.522	0.547	0.78
ratio $K_{pp}/K_{AA} = 0.70$			

TABLE I: Compilation of our knowledge on baryon inelasticity in p+p and central Pb+Pb collisions at $\sqrt{s_{NN}} = 17.27$ GeV. The value in the middle column includes both net protons and net neutrons as described in the text.

in the collisions [18], which gives $K_{pp} \approx 0.5$. It is to be noted that the $p + p \rightarrow pX$ distribution, best known experimentally, may be subject to isospin effects if compared to Pb+Pb reactions where more neutrons participate than protons. Both statements can at present be verified with experimental data from the NA49 [17] and NA61/SHINE [19] collaborations. In particular, the NA49 reference [17] includes not only precise, double differential in (x_F, p_T) , very wide acceptance proton and antiproton data, but also the neutron x_F distribution at $\sqrt{s} = 17.27$ GeV. The cited paper includes also a precise numerical interpolation of the p and \bar{p} data [14] which can be used to obtain a model-independent evaluation of net proton inelasticity. We underline again the superiority of using such a wide acceptance interpolation of experimental data rather than relying on a particular model-dependent event generator. We performed this evaluation and obtained $K = 0.522$ as shown in Table I. This was made by calculating numerically the average net proton energy in an inclusive inelastic p+p event and consequently obtaining E_{inel} in Eq. (5.6):

$$E_{inel} = \frac{\sqrt{s}}{2} - \langle E_{\text{net proton}} \rangle \quad ; \quad \text{with} \quad (5.11)$$

$$\langle E_{\text{net proton}} \rangle = \frac{\int_0^1 \int_0^{p_T(\text{max})} E(x_F, p_T) \cdot \left(\frac{d^2\sigma}{dx_F dp_T} \right)_{\text{net proton}} dp_T dx_F}{\int_0^1 \int_0^{p_T(\text{max})} \left(\frac{d^2\sigma}{dx_F dp_T} \right)_{\text{net proton}} dp_T dx_F} \quad , \quad (5.12)$$

where $E(x_F, p_T)$ is the net proton energy given by its x_F and p_T , and the net proton density is obtained by the subtraction of the quoted interpolated proton and antiproton distributions:

$$\left(\frac{d^2\sigma}{dx_F dp_T} \right)_{\text{net proton}} = \left(\frac{d^2\sigma}{dx_F dp_T} \right)_p - \left(\frac{d^2\sigma}{dx_F dp_T} \right)_{\bar{p}} \quad . \quad (5.13)$$

We note that the numerical integration in Eq. (5.12) above was performed assuming $p_T(\text{max}) = 2$ GeV/c, over a grid of 1000 x 1000 sampling points.

Subsequently, on the basis of the same data interpolation as well as of the published experimental neutron x_F distribution, we estimated the (net proton)+(net neutron) spectrum assuming that neutrons have the same shape of the p_T distribution as protons at a given x_F , an assumption that should have only a small influence on the final result. Following the considerations about antineutrons made in [17], we subtracted 1.66 times (see [17]) the antiproton distribution in order to obtain the net neutron spectrum. We applied formulae strictly similar to (5.11)-(5.13), as well as the same integration sampling grid and limits. The final result for net baryons (protons+neutrons) in the final state of the p+p collision is $K_{pp} = 0.547$, as shown in Table I. We note that this result

is already free from isospin effects as it contains both isospin partners. We neglect the contribution of other baryons like Λ due to their small cross-section.

For *central Pb+Pb collisions*, we expect that the lower acceptance coverage of existing experimental distributions may induce a stronger model dependence for the estimate on K_{AA} . On the other hand, the net proton distribution in Pb+Pb collisions should be weakly affected by isospin effects due to the mixed isospin content of the lead nucleus. All in all, we consider the estimate provided by C. Blume [20], where the contribution of unmeasured baryons was estimated from the statistical hadron gas model [21] as secure enough for our study. The latter gives $K_{AA} \approx 0.78$ at top SPS energy.

From the above, we estimate from (5.9) and (5.10):

$$A_{pp}/A_{AA} = K_{pp}/K_{AA} = 0.547/0.78 \approx 0.70 \quad . \quad (5.14)$$

This is to be compared to $A_{pp}/A_{AA} = 0.812$ established from Fig. 6 in section III. Thus we see that energy conservation-related considerations connected to changes in baryon inelasticity can explain a part of the normalization difference between the experimental pion rapidity spectrum in inelastic p+p collisions, and that obtained from a single fire-streak in Pb+Pb reactions. However, our result overpredicts the difference which we saw in Fig. 6: the fire-streak fragmentation function matches the shape of the experimental $p + p \rightarrow \pi^- X$ spectrum, but the difference in the absolute normalization of the two distributions is *smaller* than what is expected solely from differences in inelasticity.

B. Strangeness enhancement

It is very well known that production of strange particles (mostly K mesons [9], but also strange baryons [22]) is significantly enhanced in Pb+Pb with respect to p+p collisions. In the following we refrain from discussing the dynamical origin of strangeness enhancement which has been done before in very well known papers [7, 8]. We focus on the energy balance between strange and non-strange particle production. For simplicity we limit ourselves to pions and kaons which dominate the yields of produced particles. The changes in baryon inelasticity must also be taken into account.

Table II displays our compilation of kaon and pion yields in central Pb+Pb as well as p+p collisions, taken together with mean pion and kaon energies in inelastic p+p events at the top SPS energy. The latter should be commented upon. The presented estimates are in our view completely model-independent as they are uniquely based on very detailed and wide acceptance two-dimensional (x_F, p_T) distributions from the NA49 experiment [4, 24]. Precise numerical interpolations of these distributions have been included therein and remain available in [14]. Our estimates for mean energies are directly, numerically computed from these interpolated experimental distributions. For this purpose we use a formula similar to (5.12):

$$\langle E_i \rangle = \frac{\int_0^1 \int_0^{p_T(\max)} E_i(x_F, p_T) \cdot \left(\frac{d^2\sigma}{dx_F dp_T} \right)_i dp_T dx_F}{\int_0^1 \int_0^{p_T(\max)} \left(\frac{d^2\sigma}{dx_F dp_T} \right)_i dp_T dx_F} \quad , \quad (5.15)$$

where i denotes the particle type ($i = \pi^+, \pi^-, K^+, K^-$), for which the production cross section $\left(\frac{d^2\sigma}{dx_F dp_T} \right)_i$ has been measured and numerically interpolated over a very large

Reaction	total average yield per event			
	π^+	π^-	K^+	K^-
central Pb+Pb, $\sqrt{s_{NN}} = 17.27$ GeV	560 [23]	602 [5]	97.8 [5]	54.0 [5]
inelastic p+p, $\sqrt{s_{NN}} = 17.27$ GeV	3.018 [4]	2.360 [4]	0.2267 [24]	0.1303 [24]
	average energy per particle [MeV]			
	905	781	1388	1107

TABLE II: Charged pion and kaon yields in central Pb+Pb and inelastic p+p collisions at top SPS energy, put together with our estimates of mean pion and kaon energy in inelastic p+p collisions obtained numerically from interpolated experimental data as discussed in the text. The quoted values are taken from the references cited in the table.

phase space in [4, 24]. $E_i(x_F, p_T)$ denotes the particle's energy at a given (x_F, p_T) which is uniquely defined by its mass ($m_i = m_\pi$ or m_K). Thanks to the symmetry of the p+p collision we can limit the integration to positive x_F only. We apply $p_T(\text{max}) = 2$ GeV/c, and a grid of 1000 x 1000 sampling points. Here we wish to emphasize again the value of these precisely interpolated data provided by [4, 17, 24], as well as the advantage of our model-independent approach with respect to both model simulations as well as simple analytical parametrizations of experimental data.

In the following we will assume

$$\begin{aligned} \pi^0 &\approx \frac{\pi^+ + \pi^-}{2} , \\ K^0 + \bar{K}^0 &\approx K^+ + K^- \end{aligned} \quad (5.16)$$

for these particles' kinematical spectra and average yields; we consider these rough assumptions to be good enough for our present evaluation. On that basis, from Table II we obtain the average total energy which an inelastic p+p collision will spend on pion, K^+ , K^- and $(K^0 + \bar{K}^0)$ production. These we denote as $E(pp \rightarrow \pi)$, where $\pi \equiv (\pi^+ + \pi^- + \pi^0)$, and then respectively $E(pp \rightarrow K^+)$, $E(pp \rightarrow K^-)$, and $E(pp \rightarrow K^{0\bar{0}})$ where $K^{0\bar{0}} \equiv (K^0 + \bar{K}^0)$.

$$\begin{aligned} E(pp \rightarrow \pi) &= 3/2 \cdot (3.018 \cdot 905 + 2.360 \cdot 781) = 6862 \text{ MeV} , \\ E(pp \rightarrow K^+) &= 0.2267 \cdot 1388 = 315 \text{ MeV} , \\ E(pp \rightarrow K^-) &= 0.1303 \cdot 1107 = 144 \text{ MeV} , \\ E(pp \rightarrow K^{0\bar{0}}) &= 315 + 144 = 459 \text{ MeV} . \end{aligned} \quad (5.17)$$

As we consider the above values to be useful for future studies, we include them in Table III together with values of kaon/pion ratios in p+p and central Pb+Pb reactions extracted from Table II on the basis of assumptions (5.16). In addition, we calculate the ratios of energy spent on kaons (K^+ , K^- and $K^0 + \bar{K}^0$) relative to that spent on pions ($\pi^+ + \pi^- + \pi^0$) in p+p reactions and in central Pb+Pb collisions. These are respectively:

Reaction	kaon/pion ratios			
	K^+/π	K^-/π	$(K^0 + \bar{K}^0)/\pi$	
central Pb+Pb, $\sqrt{s_{NN}} = 17.27$ GeV	0.0561	0.0310	0.0871	
inelastic p+p, $\sqrt{s_{NN}} = 17.27$ GeV	0.0281	0.0162	0.0443	
	average energy per particle type [MeV]			
	$E(pp \rightarrow \pi)$	$E(pp \rightarrow K^+)$	$E(pp \rightarrow K^-)$	$E(pp \rightarrow K^{0\bar{0}})$
	6862	315	144	459

TABLE III: Kaon over pion ratios in central Pb+Pb and inclusive inelastic p+p reactions, and average energies spent on pion and kaon production in a single inelastic p+p event. By pion (π) the summed π mesons ($\pi^+ + \pi^- + \pi^0$) are meant.

$$R_{\text{energy}}(pp \rightarrow K^+/\pi) = \frac{E(pp \rightarrow K^+)}{E(pp \rightarrow \pi)} = \frac{315 \text{ MeV}}{6862 \text{ MeV}} = 0.04590 \quad , \quad (5.18)$$

$$R_{\text{energy}}(pp \rightarrow K^-/\pi) = \frac{E(pp \rightarrow K^-)}{E(pp \rightarrow \pi)} = \frac{144 \text{ MeV}}{6862 \text{ MeV}} = 0.02099 \quad , \quad (5.19)$$

$$R_{\text{energy}}(pp \rightarrow K^{0\bar{0}}/\pi) = \frac{E(pp \rightarrow K^{0\bar{0}})}{E(pp \rightarrow \pi)} = \frac{459 \text{ MeV}}{6862 \text{ MeV}} = 0.06689 \quad , \quad (5.20)$$

$$R_{\text{energy}}(pp \rightarrow \text{all kaons}/\pi) = 0.04590 + 0.02099 + 0.06689 = 0.13378 \quad , \quad (5.21)$$

$$R_{\text{energy}}(PbPb \rightarrow K^+/\pi) = \frac{\frac{K^+}{\pi}(PbPb)}{\frac{K^+}{\pi}(pp)} \cdot R_{\text{energy}}(pp \rightarrow K^+/\pi) = 0.09164 \quad , \quad (5.22)$$

$$R_{\text{energy}}(PbPb \rightarrow K^-/\pi) = \frac{\frac{K^-}{\pi}(PbPb)}{\frac{K^-}{\pi}(pp)} \cdot R_{\text{energy}}(pp \rightarrow K^-/\pi) = 0.04017 \quad , \quad (5.23)$$

$$R_{\text{energy}}(PbPb \rightarrow K^{0\bar{0}}/\pi) = \frac{\frac{K^0 + \bar{K}^0}{\pi}(PbPb)}{\frac{K^0 + \bar{K}^0}{\pi}(pp)} \cdot R_{\text{energy}}(pp \rightarrow K^{0\bar{0}}/\pi) = 0.13152 \quad , \quad (5.24)$$

$$R_{\text{energy}}(PbPb \rightarrow \text{all kaons}/\pi) = 0.09164 + 0.04017 + 0.13152 = 0.26333 \quad . \quad (5.25)$$

We note that in Eqs. (5.22)-(5.24) above, we make the important assumption that the ratio of average energy of one kaon over that of one pion remains constant between inelastic p+p and central Pb+Pb collisions. This assumption, which we consider good enough for our present evaluation, calls for an experimental verification. However, we note that as this requires a precise knowledge of $d^2n/dydp_T(y, p_T)$ distributions over a very wide range of both y and p_T , a model-independent evaluation of these quantities in Pb+Pb collisions seems difficult on the level of accuracy attainable for the p+p data, summarized by Eq. (5.17). Under this assumption we see that the kaon contribution to the overall energy balance, evaluated with respect to that of pion emission, changes by a factor of about two: from 13% in inelastic p+p to 26% in central Pb+Pb reactions.

C. Energy balance in particle emission

We will now estimate the basic balance of energy in the emission of strange and non-strange particles in the final state of p+p and Pb+Pb reactions. This we will do to investigate whether it can explain the differences in the absolute pion yield between the experimental spectrum in p+p collisions and the fire-streak fragmentation function which we obtained from the Pb+Pb data (sections III and IV). In p+p collisions, the inelastic energy (difference between baryon energy in the initial and the final state) writes:

$$E_{inel} \approx (\text{pion energy}) + (\text{kaon energy}) \quad , \quad (5.26)$$

where by “ \approx ” we mean that we neglect particles not considered in our discussion, i.e., mainly baryon and anti-baryon pairs as well as strange baryons (mainly Λ). We justify this assumption by the approximate character of our evaluation. Furthermore, we state that our estimated overall energy balance in inelastic p+p collisions holds within 3.7% even when we omit the above particles. The corresponding estimate, and a demonstration of even better consistency after the inclusion of non-strange baryon-antibaryon pairs, are presented in Appendix A.

Account taken of the quantitative relations described in sections V A and V B (formula (5.21)), Eq. (5.26) writes:

$$E_{inel}(K = 0.547) \approx (\text{pion energy}) \cdot (1 + 0.13378) \quad , \quad (5.27)$$

where K is the baryon inelasticity obtained in section V A. In central Pb+Pb collisions, from formula (5.25) the corresponding energy balance writes:

$$E_{inel}(K = 0.78) \approx (\text{pion energy}) \cdot (1 + 0.26333) \quad , \quad (5.28)$$

where the left term is given by the change in baryon inelasticity and the right term by the strangeness enhancement.

Thus the inelastic energy “lost” by one incoming baryon and spent on pion production changes from p+p to central Pb+Pb collisions. It increases by the enhancement of baryon inelasticity but then decreases by the different sharing between pions and particles containing strange quarks. The overall change of energy spent on pion production can thus be described as:

$$\frac{\text{Energy spent on pions in Pb+Pb}}{\text{Energy spent on pions in p+p}} = \frac{0.78/(1 + 0.26333)}{0.547/(1 + 0.13378)} = 1.280 = \frac{1}{0.781} \approx \frac{1}{0.70} \cdot 0.9 \quad , \quad (5.29)$$

where the last transformation states explicitly the terms induced by the change in inelasticity (section V A) and by the strangeness enhancement (section V B).

D. Normalization of pion emission in p+p and Pb+Pb collisions

Now let us calculate the relative normalization of the pion rapidity distribution in p+p collisions, with respect to that of the fire-streak fragmentation function obtained from the Pb+Pb data (Fig. 6). Eqs. (5.27), (5.28) quantify the fact that the amount of inelastic energy available for particle production, and its sharing between the emission of particles

containing and not containing strange quarks, are both different in p+p and Pb+Pb collisions. Consequently, Eqs. (5.4)-(5.5), (5.7)-(5.8), and (5.9)-(5.10) get rewritten in a new form which explicitly takes both issues into account. This gives respectively the formulae (5.30)-(5.31), (5.32)-(5.33), and (5.34)-(5.35), presented below.

$$\frac{dn}{dy}(Pb + Pb) = A_{AA}(K_{AA}, EnergySharing_{AA}) \cdot B_M \cdot (\sqrt{s} - 2m_p) \cdot F_{AA}(y) , \quad (5.30)$$

$$\frac{dn}{dy}(p + p) = A_{pp}(K_{pp}, EnergySharing_{pp}) \cdot B_M \cdot (\sqrt{s} - 2m_p) \cdot F_{AA}(y) , \quad (5.31)$$

$$\frac{dn}{dy}(p + p) = B_M \cdot \tilde{A} \cdot EnergySharing_{pp} \cdot 2E_{inel} \cdot F_{AA}(y) , \quad (5.32)$$

$$\frac{dn}{dy}(Pb + Pb) = B_M \cdot \tilde{A} \cdot EnergySharing_{AA} \cdot 2E_{inel} \cdot F_{AA}(y) , \quad (5.33)$$

$$A_{pp}(K_{pp}, EnergySharing_{pp}) = \tilde{A} \cdot EnergySharing_{pp} \cdot K_{pp} , \quad (5.34)$$

$$A_{AA}(K_{AA}, EnergySharing_{AA}) = \tilde{A} \cdot EnergySharing_{AA} \cdot K_{AA} . \quad (5.35)$$

In the formulae above, the normalization of the pion $\frac{dn}{dy}$ distribution is now a function of both the baryon inelasticity K and of the sharing of the available inelastic energy. The quantity $EnergySharing$ describes the part of this available energy spent on pions. \tilde{A} is a constant factor. Following section V C, $EnergySharing$ is respectively:

$$\begin{aligned} EnergySharing_{pp} &\approx 1/(1 + 0.13378) , & \text{from Eq. (5.27), for p+p collisions,} \\ EnergySharing_{AA} &\approx 1/(1 + 0.26333) , & \text{from Eq. (5.28), for Pb+Pb collisions.} \end{aligned} \quad (5.36)$$

Thus the normalization ratio for the two distributions (5.31) and (5.30) is

$$\frac{A_{pp}}{A_{AA}} = \frac{EnergySharing_{pp} \cdot K_{pp}}{EnergySharing_{AA} \cdot K_{AA}} = 0.781 , \quad (5.37)$$

which is a direct reflection of Eq. (5.29).

Let us underline that the normalization ratio of 0.781 given above is the *only difference* between the function with which we approximated the $\frac{dn}{dy}$ distribution of negative pions in p+p reactions (Eq. (5.2), consequently (5.5) and (5.31)) and the one which we obtained for the fire-streak in Pb+Pb collisions (Eq. (2.1), consequently (5.4) and (5.30)). This value of 0.781 has been deduced solely from our estimates of the energy balance between pion, kaon and baryon emission in p+p and in Pb+Pb events. These latter estimates have been obtained directly from interpolated experimental data on π^\pm , K^\pm , net p , and n production, with only a minimal set of basic assumptions in sections V A, V B, and V C.

The value of 0.781 is now to be compared with the factor 0.812 which we found from the comparison of our function $f(y)$ to the isospin-corrected π^- rapidity distribution in

Fig. 6, and subsequently stated in Eq. (5.3). This gives us a 4% agreement which we consider as very good, account taken of the uncertainties inherent to our study.⁴

From the above, we find it justified to conclude that the agreement of shapes shown in Fig. 6 can now be re-interpreted as a *full overall consistency* of the experimental π^- rapidity distribution in p+p collisions with the *absolutely normalized* fire-streak fragmentation function. Indeed, directly from Eqs. (5.2) and (5.37), the following becomes true:

$$\begin{aligned} & \text{Experimental } \pi^- \text{ rapidity distribution in p+p collisions} \\ & \approx \text{fire streak fragmentation function into } \pi^- \end{aligned} \quad (5.38)$$

- up to the 4% accuracy in normalization mentioned above. This occurs once the correction for isospin effects is taken into account (Eq. (4.1)), and another correction for strangeness enhancement and baryon inelasticity differences between p+p and Pb+Pb reactions is included in the comparison (Eq. (5.37)). We will further discuss these issues in section VI.

E. Comment on Eq. (5.30)

For completeness and clarity of the discussion made in section VI, below we rewrite formula (5.30) in the form evident from Eq. (5.35):

$$\frac{dn}{dy} = \tilde{A} \cdot \text{EnergySharing} \cdot K \cdot B_M \cdot (\sqrt{s} - 2m_p) \cdot \exp\left(-\frac{[y^2 + \epsilon^2]^{\frac{1}{2}}}{r \cdot \sigma_y^r}\right). \quad (5.39)$$

In the above we dropped all the reaction-specific indices and wrote explicitly the shape factor introduced in Eq. (5.4). The parameters ϵ , σ_y , and r are obtained from the fit to Pb+Pb collisions (section II), and $\tilde{A} = 0.0907$ from Eq. (5.35). The formula (5.39) gives our fire-streak fragmentation function in central Pb+Pb collisions, at $b = 0$. After the correction for strangeness suppression in p+p relative to Pb+Pb collisions and for the difference in baryon inelasticity (parametrized respectively by *EnergySharing* and K), the same formula gives the blue curve which approximately describes the isospin corrected p+p data points in Fig. 6 (within 4% accuracy as discussed in section V D).

VI. DISCUSSION

In this section we will attempt to draw the conclusions from the findings made in the present study, partially in the context of these made in our earlier work [1].

Our initial concept [1], with some similarity to the fire-streak picture [2], was introduced in order to explain the role of geometry and local energy-momentum conservation in the centrality dependence of Pb+Pb collisions at SPS energies. Simultaneously, our work [1] was inspired by, and meant to explain, our observations from spectator-induced

⁴ We note that the latter include both our assumptions and approximations as well as the uncertainties of the experimental p+p and Pb+Pb data which we used. For instance, the systematic errors of the experimental pion dn/dy yields in Pb+Pb collisions reach 5-10% depending on centrality [5].

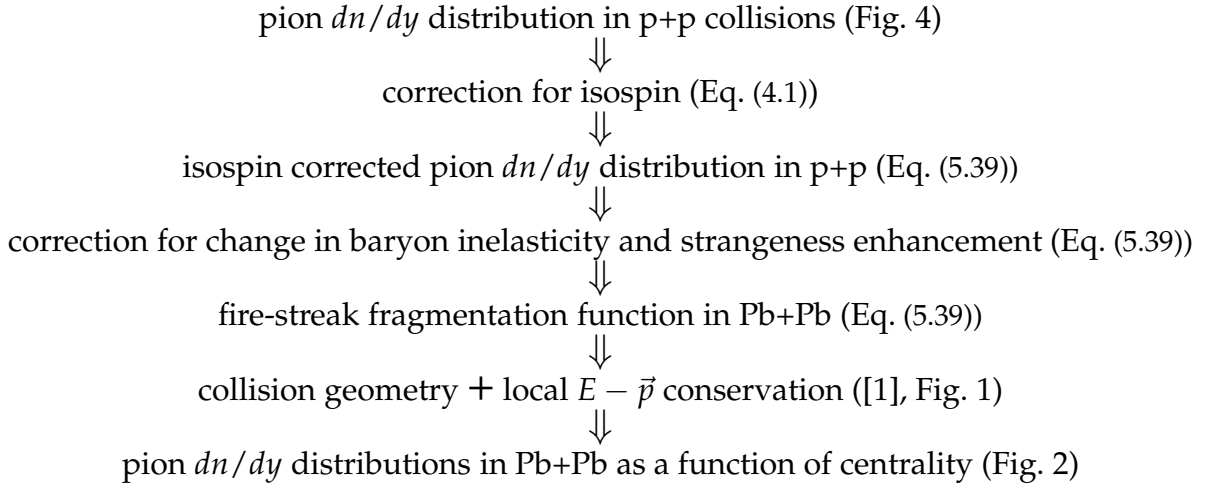
electromagnetic effects on π^+/π^- ratios and directed flow in heavy ion collisions [25–28], indicating that pions at higher rapidity are produced closer to the spectator system as it is suggested by Fig. 1.

The result was that the full centrality dependence of pion rapidity distributions and total pion yields could be understood from three elements: (a) collision geometry (b) local energy-momentum conservation, and (c) our simple fire-streak fragmentation function, producing pions proportionally to the available energy (Eq. (2.1)).

With the present work, however, a new element appears in the picture which is the (exact or approximate) consistency of the isospin corrected experimental π^- rapidity distribution in p+p reactions with the fire-streak fragmentation function, as shown in Fig. 6 and stated in section V D. This consistency emerges *only* when the normalization of the latter is corrected for the change in baryon inelasticity and the strangeness enhancement between p+p and Pb+Pb collisions. This brings specific implications, some of which we will point below.

A. Pion rapidity spectra

In the present study, one component of our successful description of pion production in Pb+Pb reactions from Ref. [1] - the fire streak fragmentation function - appears “available” in p+p collisions once the effects of baryon inelasticity and strangeness suppression are taken into account. Thus one can think of the following simple “prescription” to follow in order to describe, or parametrize, the centrality dependence of pion rapidity distributions and their total yields in Pb+Pb reactions, starting from p+p collisions:



We underline that the scheme above may be followed both “down” and “up”. For instance, our study made in Ref. [1] supplemented by the present analysis, follows it “up” from the centrality dependence of the Pb+Pb reactions up to the pion spectrum in p+p collisions. The prescription established above will keep track of the whole shape evolution of the dn/dy distribution from p+p through peripheral up to central Pb+Pb collisions, and of the relative increase of pion multiplicity as a function of decreasing impact parameter of the Pb+Pb collision. In our view, this “correspondence” between rapidity distributions in p+p and Pb+Pb interactions established by our prescription brings additional support to our simple picture of the longitudinal evolution of the Pb+Pb system. In

this picture, finite size volumes of deconfined primordial matter initially move following local energy-momentum conservation, and a number of mechanisms resulting in production of final state particles in Pb+Pb collisions (dressing up of quarks into hadrons, etc) preserve some degree of similarity to p+p reactions.

B. Differences between p+p and Pb+Pb collisions

As a continuation of our paper [1], the present work is aimed at pointing out possible common points and similarities in pion rapidity distributions for the two reactions. Its limitations should also be pointed out. Evidently, our work does not genuinely “explain” strangeness enhancement nor the changes in inelasticity K between proton-proton and nucleus-nucleus collisions. Both of these we had to estimate from experimental data in section V for the purpose of formula (5.39). Specifically, our “correction” for strangeness suppression in p+p or strangeness enhancement in Pb+Pb reactions, introduced by the estimated quantity *EnergySharing* in Eq. (5.39), is in fact a simple “translation” of enhanced strange particle yields into the overall energy balance of particle production. The origin of this correction - the enhanced abundance of strange quarks in the deconfined matter produced in Pb+Pb collisions - is an independent dynamical phenomenon explained elsewhere [7]. It evidently modifies the overall energy balance in particle emission but it is only parametrized in our study. As such, no claim can be made about bulk properties of heavy ion collisions being predictable solely from p+p reactions on the basis of the present work.

Also, in our view, our results do not point towards the applicability of the geometrical picture of many fire-streaks, as drawn in Fig. 2, to proton-proton reactions. This is in contrast to our work on pion dn/dy distributions in Pb+Pb collisions [1]. The fact that consistency can be found between the experimental pion rapidity distribution in p+p collisions and the fragmentation function of the *single* fire-streak, rather than a *sum* of fire-streaks, would suggest a difference between the two reactions. While Pb+Pb data can be described by a superposition of many independent fire-streaks, only a single fire-streak would be formed in the p+p collision.

VII. SUMMARY

In the present paper we investigated to which extent the phenomenological rapidity distribution of pions from the fire-streak in Pb+Pb collisions, extracted recently, is similar to the pion rapidity distribution in p+p collisions. With no tuning nor adjustment to experimental data, our single fire-streak pion $\frac{dn}{dy}$ distribution obtained from Pb+Pb reactions reproduced the shape of the experimental pion rapidity spectrum in p+p interactions at the same energy. Isospin differences between Pb+Pb and p+p collisions have been taken into account. The absolute normalization of pion spectra between the two reactions could be fully (up to 4% precision) explained by changes in the energy balance induced by baryon stopping and strangeness enhancement phenomena.

From the above we conclude that once the above phenomena are taken into account, and the influence of Pb+Pb reaction geometry as well as local energy-momentum conservation are properly considered, an interesting correspondence emerges between absolutely normalized pion rapidity spectra in inelastic p+p collisions and pion rapidity

distributions in centrality selected Pb+Pb reactions.

Acknowledgments

We gratefully thank Adam Bzdak for pointing to us the importance of the extension of our study to p+p reactions. We acknowledge the work of Hans Gerhard Fischer on the release and especially the precise numerical interpolation of NA49 proton+proton data which allowed a model-independent calculation of the energy balance in p+p collisions. We are indebted to Jan Rafelski for his remarks on the fire-streak model, and to our referees for very valuable comments and constructive criticism. This work was supported by the National Science Centre, Poland (grant number 2014/14/E/ST2/00018).

-
- [1] A. Szczurek, M. Kielbowicz and A. Rybicki, Phys. Rev. C **95**, no. 2, 024908 (2017) [arXiv:1612.06694 [nucl-th]].
 - [2] W.D. Myers, Nucl. Phys. A296 (1978) 177., see also:
R. Hagedorn, Thermodynamics of Strong Interactions, CERN 71-12.
J. Gosset, J.I. Kapusta and G.D. Westfall, Phys. Rev. C18 (1978) 844.
V.K. Magas, L.P. Csernai and D.D. Strottman, Phys. Rev. C64 (2001) 014901.
V.K. Magas, L.P. Csernai and D.D. Strottman, Nucl. Phys. A712 (2002) 167.
I.N. Mishustin and J.I. Kapusta, Phys. Rev. Lett. 88 (2002) 112501.
 - [3] S. Kretzer, E. Leader and E. Christova, Eur. Phys. J. C **22**, 269 (2001) [hep-ph/0108055].
 - [4] C. Alt *et al.* [NA49 Collaboration], Eur. Phys. J. C **45**, 343 (2006) [hep-ex/0510009], and references therein.
 - [5] T. Anticic *et al.*, Phys. Rev. C **86**, 054903 (2012).
 - [6] S. Afanasiev *et al.* [NA49 Collaboration], Phys. Rev. C **66**, 054902 (2002),
C. Alt *et al.* [NA49 Collaboration], Phys. Rev. C **77**, 024903 (2008).
 - [7] J. Rafelski and B. Müller, Phys. Rev. Lett. **48**, 1066 (1982).
 - [8] M. Gazdzicki and M. I. Gorenstein, Acta Phys. Polon. B **30**, 2705 (1999) [hep-ph/9803462].
 - [9] A. Aduszkiewicz [NA61/SHINE Collaboration], Nucl. Phys. A **967**, 35 (2017), arXiv:1704.08071 [hep-ex].
 - [10] J. Adam *et al.* [ALICE Collaboration], Nature Phys. **13**, 535 (2017), arXiv:1606.07424 [nucl-ex].
 - [11] V. Ozvenchuk and A. Rybicki, Nucl. Phys. A **973**, 104 (2018), arXiv:1711.02963 [hep-ph].
 - [12] L. Adamczyk *et al.* [STAR Collaboration], Nature **548**, 62 (2017), arXiv:1701.06657 [nucl-ex], and references therein.
 - [13] Y. Xie, D. Wang and L. P. Csernai, Phys. Rev. C **95**, no. 3, 031901 (2017), arXiv:1703.03770 [nucl-th], and references therein.
 - [14] <https://spshadrons.web.cern.ch/spshadrons>
 - [15] O. Chvala, NA49 Collab., Eur. Phys. J. C **33** (2004) S615.
 - [16] W. Busza and A. S. Goldhaber, Phys. Lett. **139B**, 235 (1984).
 - [17] T. Anticic *et al.* [NA49 Collaboration], Eur. Phys. J. C **65**, 9 (2010) arXiv:0904.2708 [hep-ex].
 - [18] H. Strobele [NA49 Collaboration], PoS CPOD **2009**, 044 (2009) [arXiv:0908.2777 [nucl-ex]].
 - [19] A. Aduszkiewicz *et al.* [NA61/SHINE Collaboration], Eur. Phys. J. C **77**, no. 10, 671 (2017), arXiv:1705.02467 [nucl-ex].
 - [20] C. Blume [Na49 Collaboration], J. Phys. G **34**, S951 (2007) [nucl-ex/0701042].

- [21] F. Becattini, J. Manninen and M. Gazdzicki, *Phys. Rev. C* **73**, 044905 (2006) [hep-ph/0511092].
- [22] F. Antinori *et al.* [NA57 Collaboration], *J. Phys. G* **32**, 427 (2006) [nucl-ex/0601021].
- [23] NA49 Collab., compilation of numerical results, <http://na49info.web.cern.ch/na49info/na49>
- [24] T. Anticic *et al.* [NA49 Collaboration], *Eur. Phys. J. C* **68**, 1 (2010), arXiv:1004.1889 [hep-ex].
- [25] A. Rybicki, A. Szczurek, *Phys. Rev. C* **75**, 054903 (2007).
- [26] A. Rybicki and A. Szczurek, *Phys. Rev. C* **87**, 054909 (2013).
- [27] A. Rybicki, A. Szczurek and M. Kłusek-Gawenda, *Acta Phys. Polon. B* **46**, no. 3, 737 (2015).
- [28] A. Rybicki *et al.*, *Acta Phys. Polon. Supp.* **9**, 303 (2016).
- [29] D. Varga [NA49 Collaboration], *Acta Phys. Hung. A* **17**, 387 (2003) [hep-ph/0303030].
- [30] A. Bialas, A. Bzdak and V. Koch, *Acta Phys. Polon. B* **49**, 103 (2018), arXiv:1608.07041 [hep-ph].

APPENDIX A. THE ENERGY BALANCE IN P+P REACTIONS AT SPS ENERGIES

In the following we cross-check the overall energy balance in p+p reactions at the top SPS energy ($\sqrt{s}=17.27$ GeV) as emerging from our considerations made in section V. Following the approximation made therein in Eq. (5.26) we assume that the energy E_{inel} lost by the incoming baryon is spent uniquely on final state pion and kaon production. This means that we neglect the production of baryon-antibaryon pairs as well as other less abundant particles. Under this assumption the partition of energy in the final state writes:

$$\sqrt{s} \approx (\text{net baryon energy}) + (\text{pion energy}) + (\text{kaon energy}) \quad , \quad (7.1)$$

where each of the three terms corresponds to the average summed energy of all the net baryons, pions and kaons in the inelastic p+p event. Relating this to the baryon inelasticity K introduced in Eq. (5.6) we obtain:

$$\sqrt{s} \approx 2m_p + (\sqrt{s} - 2m_p) \cdot (1 - K) + (\text{pion energy}) + (\text{kaon energy}) \quad , \quad (7.2)$$

where m_p is the proton mass and the difference between the latter and the neutron mass is neglected. We assume $K = 0.547$ which we obtained for summed net protons and net neutrons in section V A; thus, we neglect the small changes in the net baryon term of Eq. (7.1), possibly induced by the presence of Λ as well as other baryons in the final state. From Eq. (5.17) we have:

$$\begin{aligned} (\text{pion energy}) &= E(pp \rightarrow \pi) = 6862 \text{ MeV} \quad , \\ (\text{kaon energy}) &= E(pp \rightarrow K^+) + E(pp \rightarrow K^-) + E(pp \rightarrow K^{0\bar{0}}) = 918 \text{ MeV} \quad , \end{aligned} \quad (7.3)$$

and Eq. (7.2) writes:

$$\sqrt{s} \approx 2 \cdot 0.938 + 15.394 \cdot (1 - 0.547) + 6.862 + 0.918 = 16.629 \text{ GeV} \quad . \quad (7.4)$$

In comparison to the original value of $\sqrt{s} = 17.27$ GeV, this gives us the 3.7% agreement mentioned in section V C, which we consider good enough taken the accuracy of the present work.

It is interesting to consider the impact of other particles, neglected in the present study, on the overall energy balance in p+p reactions. While a complete study is beyond the scope of this paper, we note that to evaluate this impact is most straight-forward for the contribution of non-strange baryon-antibaryon pairs, that is, pair produced p , \bar{p} , n , and \bar{n} . For antiprotons, precise wide-acceptance double-differential (x_F, p_T) distributions are available in p+p collisions from the NA49 experiment [17], including a precise numerical interpolation [14] as it was the case for the other particles discussed in section V. Thus we can apply formula (5.15) assuming $m_i = m_{\bar{p}}$ to estimate the mean energy of an antiproton produced in inclusive inelastic p+p collisions at $\sqrt{s} = 17.27$ GeV. We obtain:

$$\langle E_i \rangle = \langle E_{\bar{p}} \rangle = 1451 \text{ MeV} \quad . \quad (7.5)$$

Subsequently, account taken of the published average multiplicity of 0.0386 antiprotons per inclusive inelastic p+p event [17], we get the average energy spent for antiproton production:

$$E(pp \rightarrow \bar{p}) = 0.0386 \cdot 1451 = 56 \text{ MeV} \quad . \quad (7.6)$$

Following the considerations made in [17], we multiply the above by 1.66 in order to obtain the average energy spent on antineutron production. Finally we multiply the summed antiproton+antineutron contribution by two in order to get the total average energy which an inelastic p+p collision spends on pair-produced protons, neutrons, antiprotons and antineutrons:

$$E(pp \rightarrow \text{non-strange, pair-produced } B \text{ and } \bar{B}) = 2 \cdot (1 + 1.66) \cdot 56 = 298 \text{ MeV} \quad . \quad (7.7)$$

Adding the above value to the right side of Eq. (7.1) we obtain $\sqrt{s} \approx 16.927 \text{ GeV}$ in Eq. (7.4), which gives an agreement within 2% with the original value of 17.27 GeV. Thus already the inclusion of non-strange baryon and antibaryon pair production improves the accuracy of our energy balance by a factor of two. We note that a 2% accuracy seems excellent to us, and emphasizes the quality of the published experimental data on p+p collisions at SPS energies which we used in this study [4, 17, 24].

APPENDIX B. ENERGY DEPENDENCE OF THE FRAGMENTATION FUNCTION

While this paper was in principle not devoted to the energy dependence of nucleus-nucleus collisions, the completeness of the discussion requires that we comment on the comparison between Fig. 2(b) and Fig. 3 made in section I. Following section II, the numerical parameters of the single fire-streak fragmentation function providing the best description of negative pion spectra in Pb+Pb collisions at $\sqrt{s_{NN}} = 17.3$ GeV (see Fig. 2 and Eq. (2.1)) are $A = 0.05598$, $\sigma_y = 1.475$, $r = 2.55$, and $\epsilon = 0.01$. For the lower collision energy of $\sqrt{s_{NN}} = 8.8$ GeV (see Fig. 3), the corresponding single fire-streak fragmentation function obeys the parametrization given by Eq. (2.1), but with different numerical parameters: $A = 0.173$, $\sigma_y = 1.800$, $r = 4.60$, and $\epsilon = 2.203$. At the present moment we do not attribute much physical sense to the changes of each given parameter taken separately, as we anyway consider the functional shape given by the exponent in Eq. (2.1) as a purely effective approximation of a complex non-perturbative process (see also the discussion made in section III, item(3)). What we consider important is that at both collision energies the fragmentation function keeps the proportionality of the number of produced pions to the available energy, $(E_s^* - m_s)$ in Eq. (2.1). This supports energy-momentum conservation as the main basis for our model, and its connection to p+p collisions which we formulated in sections II-VI.

On the other hand, it is worthwhile to perform a direct comparison of the two fragmentation functions. This is presented in Fig. 7. Both functions are taken assuming the same available energy in the fire-streak, that is, $(E_s^* - m_s) \equiv 1$ GeV in Eq. (2.1). Thus our comparison reflects both the change in the shape of the pion rapidity distribution and the change in the number of pions produced *per one GeV of available energy*, as a function of $\sqrt{s_{NN}}$.

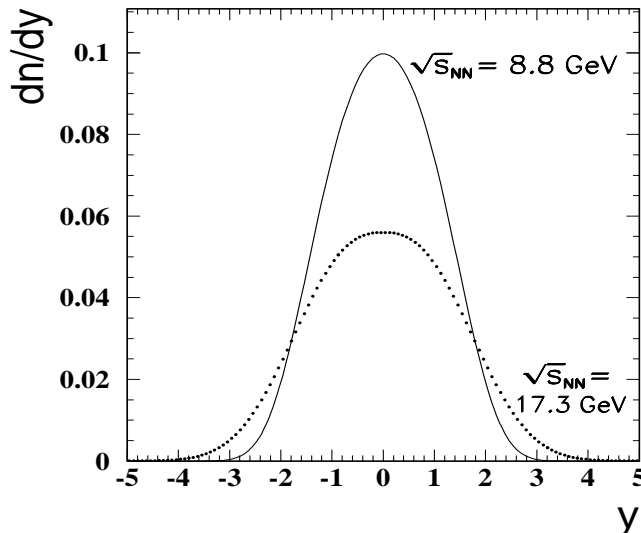


FIG. 7:

Comparison of single fire-streak fragmentation functions used for the description of π^- rapidity distributions in Pb+Pb collisions at $\sqrt{s_{NN}} = 8.8$ GeV (solid) and at $\sqrt{s_{NN}} = 17.3$ GeV (dotted).

The two presented functions are given by Eq. (2.1) with $(E_s^* - m_s) \equiv 1$ GeV. The numerical values of the function parameters are given in the text.

In our view, a consistent picture emerges from Fig. 7. With increasing collision energy, the fragmentation function broadens in rapidity, while its total integral decreases visibly. This nicely reflects the phenomenon of broadening of rapidity spectra of produced particles with increasing reaction energy, as well as the slower than linear increase of their total multiplicity as a function of \sqrt{s} .